

Special
Issue

Controlling the Uptake of Diarylethene-Based Cell-Penetrating Peptides into Cells Using Light

Tim Schober,^[a] Ilona Wehl,^[b] Sergii Afonin,^[c] Oleg Babii,^[c] Anna Lampolska,^[d, e] Ute Schepers,^[b] Igor V. Komarov,^{*[d, f]} and Anne S. Ulrich^{*[a, c]}

We report on diarylethene (DAE)-containing photoswitchable cell-penetrating peptides (CPPs) capable of photocontrolled cell entry. We demonstrate in vitro that reversible photoisomerization of a DAE fragment in the backbones of non-cytotoxic cyclic peptides influences their binding to cell membranes and subsequent CPP-mediated cargo internalization. Benign red light can be used to activate cell entry of our compounds. We suggest that the observed differences in cell uptake of the two photoisomers are due to changes in the molecular flexibility achieved upon DAE photoisomerization.

Membrane proteins that are exposed on the cell surface currently constitute the major drug targets,^[1a] but many more “druggable” biomolecules are located inside a cell.^[1b–d] Delivery of drug molecules to their specific intracellular targets could enhance therapeutic efficacy and reduce toxicity of the drugs. Accordingly, the discovery of cell-penetrating peptides (CPPs) has attracted great interest in pharmacology and medicinal chemistry, because CPPs promise to serve as universal vehicles to facilitate intracellular delivery of biologically active cargoes.^[2] Numerous structurally unrelated sequences have been demonstrated to be effective as CPPs, ranging from hydrophobic

through amphipathic to highly polar cationic peptides.^[2c] CPPs were shown to be efficient as covalent conjugates or within non-covalent assemblies with a variety of biologically active macromolecular cargoes^[2a] and nanoparticles.^[2d, e] CPPs and the ambiguities associated with their in vivo applications have been extensively reviewed.^[3]

Even 30 years after the first CPP (HIV-TAT) had been described,^[4a] no CPP-drug combination has been clinically approved.^[4b] Unfavorable pharmacokinetic characteristics of CPPs are the main reasons, as they generally possess low bioavailability due to their high polarity and susceptibility to in vivo proteolysis. Meanwhile, several design principles have been suggested to alleviate these challenges, namely: (i) peptide backbone *N*-methylation,^[5] (ii) macrocyclisation,^[6] including side-chain “stapling”,^[7] (iv) use of robust scaffolds like “knottins”,^[8] and/or (v) equipping the peptides with “chameleon” properties, i.e. dynamically exposing/shielding the uptake-promoting chemical moieties within flexible conjugates.^[9]

However, there is another major disadvantage which many CPPs intrinsically have when applied in vivo: they tend to be poorly cell-type selective. CPPs may effectively transport drugs into cells, but their unfavorable biodistribution can lead to delivery into the wrong organs and tissues, i.e. not to the desired sites of action. This may lead to an enhancement of unwanted side effects and systemic toxicity.^[4, 10]

The selectivity problem is common to many peptide-based macromolecular therapeutics. It can be tackled (i) by conjugation to targeting molecules, for example, to antibodies^[11a] (ii) by engrafting the sequence elements possessing enhanced cell-type, organ, and/or tissue-affinity,^[11b] or (iii) by developing peptides that can be selectively activated by external or internal stimuli at the desired site of action.^[12] The latter approach has been successfully applied to CPPs. For instance, charged amines or guanidinium groups in cationic CPPs have been temporarily blocked via carboxylic groups of glutamate or aspartate residues in a “charge-zipper”-like manner. The charge neutralization makes the polar CPPs cell-impermeable. Two oppositely charged peptidyl fragments in these constructs are connected through a linker that selectively degrades at a specific site in vivo, e.g., by a reducing microenvironment, by acidic hydrolysis, or by specific proteolysis in tumors.^[13] The polycationic CPP sequence released upon cleavage of the linker becomes cell-permeable, hence it can deliver a covalently conjugated cargo inside the surrounding cells.

The release of bioactive molecules triggered by various external stimuli has been extensively explored. Recently, the

[a] T. Schober, Prof. Dr. A. S. Ulrich
Karlsruhe Institute of Technology (KIT),
Institute of Organic Chemistry (IOC)
Fritz-Haber-Weg 6, 76131 Karlsruhe (Germany)
E-mail: anne.ulrich@kit.edu

[b] Dr. I. Wehl, Prof. Dr. U. Schepers
KIT, Institute of Functional Interfaces (IFG)
POB 3640, 76021 Karlsruhe (Germany)

[c] Dr. S. Afonin, Dr. O. Babii, Prof. Dr. A. S. Ulrich
KIT, Institute of Biological Interfaces (IBG-2)
POB 3640, 76021 Karlsruhe (Germany)

[d] A. Lampolska, Prof. Dr. I. V. Komarov
Taras Shevchenko National University of Kyiv,
Vul. Volodymyrska 60, 01601 Kyiv (Ukraine)

[e] A. Lampolska
Enamine Ltd., Vul. Chervonotkatska 78, 02094 Kyiv (Ukraine)

[f] Prof. Dr. I. V. Komarov
Lumobiotics GmbH
Auerstraße 2, 76227 Karlsruhe (Germany)
E-mail: igor.komarov@lumobiotics.com



Supporting information for this article is available on the WWW under <https://doi.org/10.1002/cptc.201900019>



An invited contribution to a Special Issue on Photoresponsive Molecular Switches and Machines



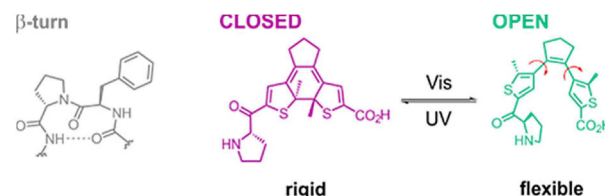
© 2019 The Authors. Published by Wiley-VCH Verlag GmbH & Co. KGaA. This is an open access article under the terms of the Creative Commons Attribution Non-Commercial License, which permits use, distribution and reproduction in any medium, provided the original work is properly cited and is not used for commercial purposes.

use of non-ionizing light for this purpose has gained particular attention, because of high spatial and temporal precision of light irradiation and its orthogonality to most biological processes.^[14] Light-activatable CPPs have been developed by several groups. For example, the concept of “photocaging”^[15] has been applied to CPPs^[16] by masking their polycationic moieties with photolabile protecting groups that deactivate cell-permeability. Subsequent irradiation with light irreversibly unmasks the charges and triggers cell entry. However, “uncaging” is problematic in vivo, because it often requires irradiation with short-wavelengths (usually UV) light. The UV light is toxic and has very low tissue penetration efficiency. For applications of light in vivo, however, the use of wavelengths within the non-toxic, tissue-penetrating optical window (red-near infrared light, wavelength 625–900 nm) is required.^[14]

Photopharmacology is a recently introduced approach to control the biological activity of compounds by the action of light, using photochromic molecules that can be reversibly isomerized.^[17] These molecules, called molecular photoswitches, undergo changes in color, geometry, flexibility, polarity or charge upon photoinduced isomerization.^[18]

There are only a few papers describing photoswitchable CPPs. Prestel and Möller used an azobenzene fragment as a photoswitchable linker between two linear polypeptide strands to photocontrol the cellular uptake.^[19] The azobenzene linker in the *cis*-configuration brought an oligoglutamate strand in close proximity to an oligoarginine sequence, promoting the formation of an intramolecular Arg-Glu-“charge-zipper” that prevents the cellular uptake. Irradiation with visible light converted the linker into the *trans*-isomer, pulling the “charge-zipper” apart and thereby triggering membrane translocation. Azobenzene-derived fragments have also been used as side chain “staples” for helical peptides, enabling photocontrol of their secondary structure and cell-entry.^[20] Nevola et al. described azobenzene-“stapled” inhibitors of a protein-protein interaction and demonstrated photoregulation of clathrin-mediated endocytosis.^[21] Recently, Kim et al. reported a cell-penetrating amphiphilic peptide that was “stapled” with an azobenzene moiety.^[22] A cell-permeable α -helix could only be formed when the azobenzene fragment was in the *cis*-configuration, so the UV-induced switch from *trans*- to *cis*-configuration promoted cell permeabilization of the peptide. This is in contrast to a construct described by Prestel and Möller,^[19] where the *cis*-isomer was less cell-permeable.

To the best of our knowledge, none of the described photocontrollable CPPs could be light-activated by wavelengths within the tissue-penetrating optical window, despite considerable progress has been made in the design of red-shifted photoswitches, for example, modified azobenzenes.^[14c,d] Aiming at practical in vivo applications of photoswitchable CPPs, we were particularly interested in using red light to promote cellular uptake. Previously, we had explored diarylethene (DAE) moieties in the backbones of cyclic peptides to photocontrol their cytotoxic activity.^[23] We have developed a DAE-based building block which mimics a β -turn element within a cyclic β -hairpin scaffold (Scheme 1). The DAE-modified β -hairpin peptides can exist in two thermally stable photoforms

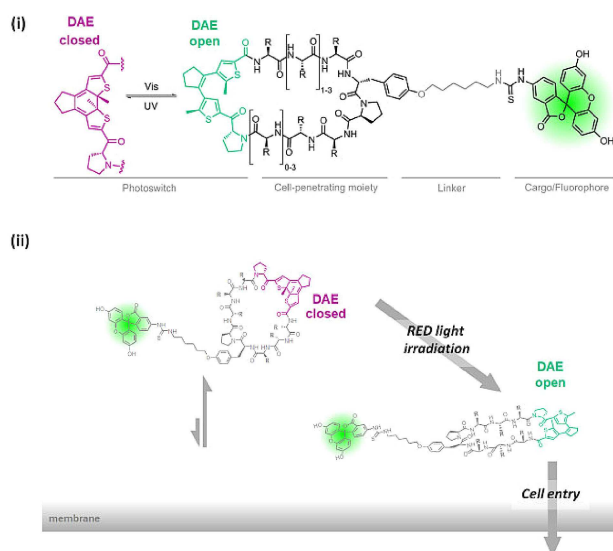


Scheme 1. The photoswitchable diarylethene (DAE)-derived amino acid building block used in this work: In comparison with a β -turn fragment.

(open and closed, Scheme 1). The open photoforms have been successfully generated by red light (wavelength in the range 617–660 nm) even in living tissues.^[23b]

Scheme 2 illustrates the general design concept which we used to construct the molecules for this study. The basic idea was to confine two short linear polypeptide strands between two turns, one being the DAE fragment, and the other one – the β -turn motif *D*-Xxx-*L*-Pro (*D*-Xxx being an α -*D*-amino acid residue, e.g. *D*-Tyr). As a cargo, we selected a fluorescein-derived fragment (to be exploited as a fluorescence reporter of the cell uptake), which was attached via a covalent linker to the tyrosyl oxygen in the β -turn. It is well-known that fluorescein as a CPP cargo might impede the cell-permeability,^[23] but we attached it to the peptide via a sufficiently long and stable linker to at least avoid the steric influence on the peptide fragment.

Due to their small ring size, the macrocycles of our constructs are relatively rigid. Hence the amino acid side chains should prefer a certain spatial geometry. This side chain arrangement and peptide dynamics can be modified upon photoisomerization of the DAE fragment.^[24] We hypothesized



Scheme 2. i) Structural template of the photoswitchable cyclic peptides explored in this study and ii) general concept of their use as red-light-triggered CPPs. The total number of amino acids in the cell-penetrating moiety and the side chains are varied (see Table 2). All peptides contain a fluorescein-derived moiety (as a cargo/fluorophore) connected through an aminohexylated tyrosine side chain (linker) to track the cell uptake. All backbone-cyclized peptides are designed to form β -hairpin structures. The photoswitch-containing fragment (colored) mimics a β -turn unit.

that such perturbation might directly influence the membrane-permeability of the molecules. Importantly, in order to use red light for switching the CPP activity on, the ability of the molecules to enter cells should be higher when the DAE fragment is converted from the closed to the open photoform. The cargo delivery would thus be triggered by light within the tissue-permeating optical window.

When choosing the amino acids to be grafted onto our macrocyclic template, we took advantage of the results published in the literature on efficient cyclic CPPs. Pei et al. developed cyclic peptides which are not only proteolytically stable and exceptionally effective as CPPs, but which can also escape endosomes and therefore can deliver cargoes all the way into the cytosol.^[25,26] Macrocyclic constructs with a tetra-arginyl fragment followed by 2–3 consecutive aromatic residues were found to outperform the known “classical” linear CPPs, such as nonaarginine (R₉), HIV-TAT, or penetratin.^[26] We also took into account the known fact that aromatic residues can form strong π - π -interactions in β -hairpins when placed onto apposing strands.^[27,28] Similarly, hydroxyl-bearing residues are known to form interstrand side chain-to-backbone hydrogen bonds in short β -hairpin-structured peptides.^[29] We reasoned that the π - π -interactions and additional hydrogen bonds could stabilize the β -stranded structure in the open photoforms, thus enhancing the efficiency of the photoswitching. Based on these literature data, we designed a series of amphipathic peptides 1–5 (Table 1).

It has been also reported that proteolytically stable and comparatively rigid cyclic oligoarginines are better CPPs than their flexible linear analogues.^[30] In line with this observation, another study had demonstrated that rigidly pre-oriented side chains bearing guanidinium groups can enhance the uptake^[31] of an oligoarginine-like polycationic CPP, provided that the distances between positive charges within the peptidomimetic matched the spacing of negative charges on membrane-exposed polyanionic glycosaminoglycans.^[32] We used these data in the design of our second series of peptides 6–8 (Table 1).

Table 1. Sequences of the studied peptides. Analogues 1–5 were designed to be amphipathic. Peptides 6–8 are oligoarginines and are therefore cationic.

Peptide	Sequence ^[a]	Cycle size ^[b]	Net charge
amphipathic series			
1	cyclo[Φ RRFy ^{Ahx} PNaIRR]	10-mer	+4
2	cyclo[Φ RRFy ^{Ahx} PWRR]	10-mer	+4
3	cyclo[Φ RRFy ^{Ahx} PFRR]	10-mer	+4
4	cyclo[Φ TRRy ^{Ahx} PRR]	9-mer	+4
5	cyclo[Φ FRRy ^{Ahx} PRR]	9-mer	+4
oligoarginine series			
6	cyclo[Φ RRRy ^{Ahx} PRRR]	10-mer	+6
7	cyclo[Φ RRRy ^{Ahx} PRRRR]	12-mer	+8
8	cyclo[Φ RRRRy ^{Ahx} PRRRRR]	14-mer	+10

[a] Φ : the DAE fragment, y^{Ahx}: O-amino-hexylated *D*-tyrosine, NaI: 2-naphthylalanine, [b] assuming Φ to be equivalent of two amino acid residues

For all experiments, the peptides 1–8 bearing the DAE moiety in the closed form were prepared and purified (for details see Supporting Information, SI). They were quantitatively converted into the corresponding open photoforms with visible light immediately before the experiments. Absorption properties and kinetics of full conversion of the closed photoforms to the corresponding open ones were studied by UV-Vis spectroscopy and HPLC in separate experiments. We found that virtually complete conversion (closed to open) can be induced by irradiation with red light (617–660 nm). Figure 1 illustrates

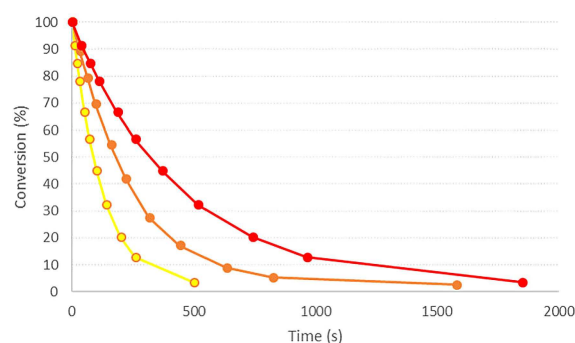


Figure 1. Time-dependent DAE-closed to DAE-open photoconversion of peptide 5 under irradiation with commercial LEDs. Yellow trace: using an LED with $\lambda_{\text{max}} = 590$ nm, orange: with $\lambda_{\text{max}} = 617$ nm, and red: with $\lambda_{\text{max}} = 660$ nm. Absorbance at 575 nm is present only in the closed DAE and is therefore used to track the amount of the closed photoform. A 50 μM solution of pure closed 5 in 50 MeOH–H₂O (50:50 v/v) was exposed to LED illumination under continuous stirring. All the graphs correspond to irradiance of ~ 25 mW/cm².

that the photoconversion rates triggered by yellow (LED $\lambda_{\text{max}} = 590$ nm), amber (LED $\lambda_{\text{max}} = 617$ nm) and deep-red (LED $\lambda_{\text{max}} = 660$ nm) light (irradiance ~ 25 mW/cm²) are high and practically similar; in most experiments described below we used yellow light due to technical reasons. Perfect isosbestic points observed in the UV-Vis spectra (see the SI) during the photoconversion indicated that the process was two-component, and that the peptides were stable during photoisomerization. No side products were detected by HPLC analysis after photo-switching.

First, we assessed the overall hydrophobicity of the peptides by measuring their chromatographic retention times (RTs) on a reversed-phase C₁₈-column with a uniform gradient (water/acetonitrile) elution. To a first approximation, RTs reflect the general hydrophobicities of the cationic molecules at low/neutral pH, and could thus be used to rank our compounds according to their predicted membrane-binding affinities.^[33] The RT values for peptides 1–8 measured under the conditions described in the literature^[34b] are listed in Table 2. As expected, the amphipathic peptides 1–5 were significantly more hydrophobic (they have longer RTs) than the arginine-rich derivatives 6–8.

Among the amphipathic peptides 1–3 (closed), the less hydrophobic ones were those where the naphthylalanine residue was replaced by Trp or Phe. Peptide 4 (closed) appeared significantly less hydrophobic than the other amphi-

Table 2. Retention times (RTs) of the pure closed and open photoforms of the CPPs 1–8 on a reversed-phase C₁₈ HPLC column (see the SI for details).

Peptide	RT (closed) [min]	RT (open) [min]	Δ RT [min]
1	34.3	40.8	6.5
2	32.1	37.4	5.3
3	32.4	37.9	5.5
4	27.7	33.4	5.7
5	32.2	34.2	2.0
6	24.8	25.5	0.7
7	22.9	23.6	0.7
8	22.1	22.6	0.5

pathic analogues, which can be explained by the presence of the polar Thr residue. Among the oligoarginine series 6–8, the more charged peptides were increasingly more polar. The open photoforms with the flexible DAE fragment that might promote structuring consistently revealed longer RTs (and, correspondingly, higher hydrophobicities) when compared to their closed isomers. This correlation gave us the confidence that photo-switching the DAE moieties in our constructs should indeed change the membrane affinities of the peptides, because hydrophobicity is the most obvious property of peptides that directly determines their strength of the initial interaction with eukaryotic cell membranes.

We noticed some interesting trends in the hydrophobicity profiles upon photoswitching when analyzing the differences between RT (open) and RT (closed) (Δ RTs, Table 2). Peptide 1 (open) is the most hydrophobic in both photoforms, with the largest Δ RT. Peptide 3 with two apposing Phe residues became more hydrophobic upon switching to the open form than peptide 2 with a corresponding Phe/Trp pair. Interestingly, compound 4 bearing Thr demonstrated the third largest Δ RT, indicating that the Thr side chain might indeed be capable of forming intramolecular hydrogen bond in the flexible (open) photoform, as we had suggested. For the arginine-rich derivatives 6–8, we observed only limited changes in the RT upon photoswitching. Obviously, the subtle changes in the structure and dynamics of the oligo-Arg backbone upon photoswitching are not sufficient to modulate overall hydrophobicity of 6–8.

As a next step, we studied the cytotoxicity of the peptides 1–8. The closed and open forms were examined separately (Figure 2). As controls in the cytotoxicity and uptake studies four FITC labelled peptides were taken: a linear oligoarginine derivative (9), a cyclic oligoarginine derivative (10), a cyclic non-photoswitchable (DAE-free) analogue of 4 (11), and non-photoswitchable linear analogue of 4 (12) (the structures are shown in SI). We used the MTT (3-(4,5-dimethylthiazol-2-yl)-2,5-diphenyl-tetrazolium bromide) assay with HeLa cells to check the cell viability after 72 h of incubation with 1–8 over a concentration range of 1–20 μ M, where “classical” CPPs are effective and arginine-rich CPPs were reported to be relatively non-toxic.^[34a] In general, the closed forms showed slightly lower cytotoxicity than the corresponding open forms. Only peptide 8 (both open and closed) with the largest number of arginine residues caused the cell viability to decrease to below 50% at 20 μ M. This result correlates with previous observations that

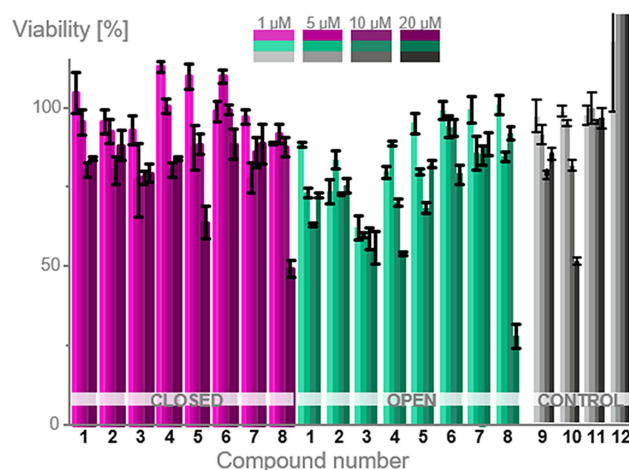


Figure 2. Cytotoxicity of the photoswitchable CPPs 1–8 and controls 9–12 assessed through an MTT assay with HeLa cells. The concentration range comprises earlier reported effective concentrations of peptides with comparable composition. Metabolic cell viability was calculated relating to the negative control (no peptide was added to the growth media).

increasing the number of arginine residues enhances the cytotoxicity of (R)_n CPPs.^[34] Lower concentrations of 8, as well as of other peptides, showed no significant toxicity at all tested concentrations for both photoforms. We observed no simple correlation between cytotoxicity and hydrophobicity. The most hydrophobic peptide 1 (open) did not show the highest cytotoxicity, whereas the most polar 8 (closed) seems to have the strongest effect on eukaryotic cell viability.

Finally, the uptake of the peptides into eukaryotic cells was examined. We used confocal fluorescence microscopy to assess whether our peptides are cell-penetrating, and if so, whether there are any differences in the uptake efficiency between the open and closed forms. Pure closed forms of the peptides were used as starting stock solutions and were switched to the open forms with visible light ($\lambda = 590$ nm) before adding them to the cells. We used the same concentration range 1–20 μ M as in the toxicity experiments, but the incubation time was less (3 h instead of 72 h) to ensure less cytotoxicity. After co-incubation with peptides, trypan blue (TB)^[35] was added to the extracellular medium to quench the fluorescence of the non-internalized peptides. A representative set of experimental data is shown in Figure 3. As can be seen, all our peptides showed detectable uptake within the tested concentration range. Figure 4 shows magnified images of the cells treated with representatives of the two series [4 (open), and 8 (open)]. No nuclear delivery is evident, as there is no apparent co-staining with the nuclear dye.

For the oligoarginine derivatives 7–8 and peptide 2 we could not detect any significant difference in uptake between the closed and open forms. However, we were pleased to see that for peptide 6 and the amphipathic peptides 1, 3–5 an increased uptake of the open forms was observed. This finding justifies the design and suggests that compounds 1–5 could be a good starting point for the development of drug delivery systems in vivo, because the open forms, as pointed out earlier, can be generated by benign red light. The control linear

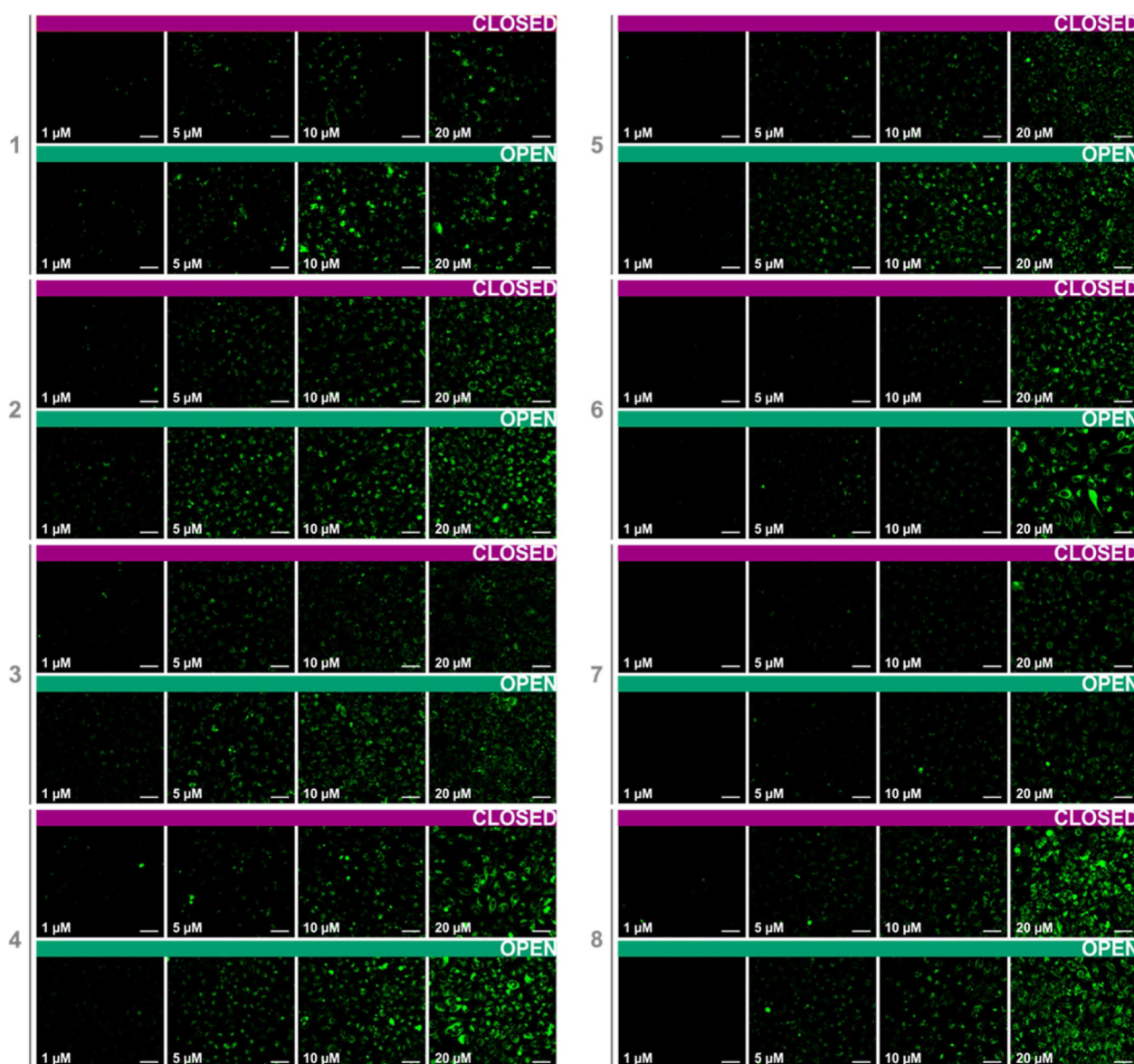


Figure 3. Confocal microscopy images displaying concentration-dependent uptake in live HeLa cells. The scale bars are 50 μm . Cells (1.5×10^4 per well) were incubated for three hours at 37 $^{\circ}\text{C}$ with the peptides at the indicated concentration, washed three times before TB was added to quench the non-internalized fluorescence. Stained nuclei and brightfield pictures are omitted for clarity. Open forms were prepared in situ with 590 nm light to ensure the concentrations of the corresponding peptide photoforms were identical.

oligoarginine peptide **9** showed relatively low uptake while the cyclic oligoarginine **10** demonstrated much better CPP activity at a level similar to the photoswitchable oligoarginine **8**. On the other hand, controls **11** and **12** (cyclic and linear non-photoswitchable analogues of **4**, correspondingly) did not show any observable uptake, most probably because they do not have an amphipathic β -hairpin structure (**12** is a truncated 9-mer).

In this study, we were primarily interested in demonstrating an effect of peptide photoswitching on intracellular uptake. Hence, we quantified relative fluorescence intensities on the images obtained at 5 μM peptide concentration using *ImageJ*. The results are summarized in Figure 5. Peptide **4** showed the largest uptake difference, followed by **1** and **5**.

A closer look at the images revealed large fluorescent patches, which cannot be assigned to any cellular structure. We attribute these patches to extracellular peptide aggregates that could not be completely quenched with TB (see Figure 6).

Comparing the cellular uptake results with the HPLC RTs and the data of the MTT assays, no clear correlations between hydrophobicity, toxicity and uptake assessed by the fluorescence intensity were found for the whole peptide set **1–8**. However, some trends could be identified within the two peptide series, **1–5** and **6–8**. Oligoarginine peptides **6–8** did not change hydrophobicity upon photoswitching, and below 10 μM did not reveal significant changes in cytotoxicity upon switching; peptides **7–8**, but not **6**, were taken up to a similar extent in both photoforms. The difference in uptake of the

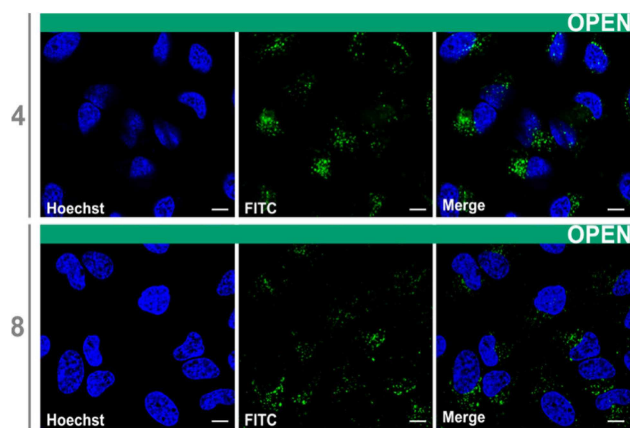


Figure 4. Magnified view of the HeLa cells incubated with peptides 4 and 8 at 5 μM concentration to visualize the fluorophore cellular localization. Nuclei were stained with Hoechst. The scale bars are 10 μm .

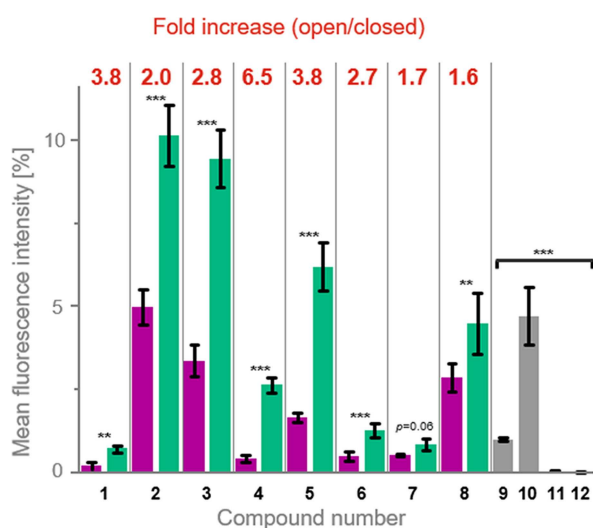


Figure 5. Fluorescence intensity of the open and closed photoforms of the peptides 1–12 and the ratio between open and closed forms for the photoswitchable peptides 1–8 penetrated into HeLa cells. Microscopy data from the cells exposed to 5 μM peptide solutions for three hours at 37 $^{\circ}\text{C}$ in the growth media after TB quenching was used. Ten to seventeen frames from at least three different locations were averaged. Statistical analysis was done with one-way ANOVA, relating to the closed/open ratio of peptide 1 and within the control peptide series. * $P < 0.05$, ** $P < 0.01$, and *** $P < 0.005$.

smallest peptide 6, however, suggests that the changes in backbone flexibility (upon photoswitching of the DAE moiety) are not sufficient to affect the larger polycationic macrocycles. Fortunately, our concept worked better for the less charged amphiphilic peptides 1–5. Here, we observed that photoisomerization-driven changes in macrocycle backbone structure and dynamics can influence the cell penetrability in the desired way: the more flexible open forms were consistently more active, as had been observed also with other bioactive DAE-derived peptidomimetics.^[36] Peptides 1–3 were designed to benefit in the open form from backbone structuring by aromatic π - π -interactions between Phe/Nal, Trp/Phe and Phe/Phe residues, whereas peptide 5 was a control. Judging from ΔRTs (Table 2), the control peptide indeed exhibits less

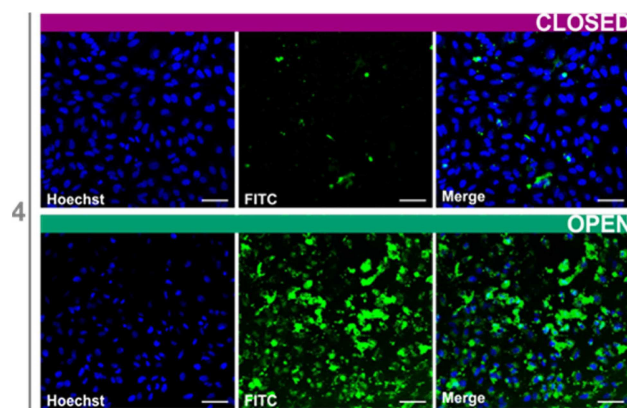


Figure 6. Fluorescence images of peptide 4 at 5 μM without extracellular fluorescence quenching by Trypan Blue. The scale bars are 50 μm . Clusters of bright green patches corresponding to extracellular fluorescence can be observed.

structuring upon photoisomerization, and 1–3 could be ranked as 1 > 3 > 2. The Trp analogue 2 did not demonstrate a big change in hydrophobicity or uptake efficiency upon photo-switching, hence the order remained. However, the control peptide 5 appeared to show more photoswitchable uptake, exceeding the differences between the two photoforms of peptides 2 and 3. On the other hand, peptide 4 seems to perform as expected – the high ΔRT values translated into large uptake differences. The most hydrophobic naphthylalanine-containing analogue 1 had the largest difference in retention time (i.e. was most structured in the open form) but presumably was less effective in the cellular uptake assay as it suffered from extracellular aggregation. Indeed, we noticed differences in the images when performing the uptake experiments with and without TB quenching for all amphipathic peptides. Figure 6 illustrates the fluorescence difference for peptide 4 in such case (compare to Figure 3). At first glance, the photoswitching effect appears to be pronounced in Figure 6, however, it is evident that a large fraction of the fluorescence has to be assigned to extracellular peptide.

It appears that in more hydrophobic macrocycles the DAE-photoisomerization affects not only the cell permeability, but even more so the polarity-driven affinity of the peptides to the membrane surface, as well as their ability to self-aggregate. Accordingly, the open forms have a higher membrane binding affinity, but they also aggregate more vigorously – presumably due to their increased hydrophobicity. Any subsequent internalization does not occur (for the fraction remaining in the large extracellular aggregates). It is also possible that aggregated entities undergo different internalization pathways, compared to monomeric species.^[37]

In summary, we have synthesized 8 fluorescein-labelled photoswitchable cyclic cell-penetrating peptides with varying size and amino acid composition and 4 non-photoswitchable controls. Two photoforms of these peptides showed different retention times in reversed-phase HPLC, with the open form isomers being consistently more hydrophobic. The peptides did not show significant cytotoxicity at concentrations < 10 μM .

Except for two oligoarginine analogues, all peptides were well taken up into HeLa cells at a concentration of 5 μ M in their open forms. All open forms showed at least to some extent a higher uptake than the respective closed forms. Peptide 4 demonstrated 6.5 fold difference in intracellular fluorescence intensity. Notably, we could demonstrate here that photo-switching to the more cell-permeable compounds can be achieved by red light in cyclic peptides that were modified with a DAE fragment.

Acknowledgements

T.S., I.W., S.A., U.S., and A.S.U. acknowledge funding from KIT, the state of Baden-Württemberg, and the German Research Foundation (DFG) through GRK 2039 "Molecular architecture for fluorescent cell imaging". T.S., S.A., O.B., A.I., I.V.K. and A.S.U. acknowledge EU funding by the EU H2020-MSCA-RISE through the PELICO project (grant 690973). A.S.U. and O.B. acknowledge the Federal Ministry of Education and Research (BMBF) for the VIP-PLUS funding.

Conflict of Interest

The authors declare no conflict of interest.

Keywords: cell-penetrating peptides • cell uptake • diarylethenes • photopharmacology • photoswitches

- [1] a) J. P. Overington, B. Al-Lazikani, A. L. Hopkins, *Nature Rev. Drug Discov.* **2006**, *5*, 993–996; b) A. L. Hopkins, C. R. Groom, *Nat. Rev. Drug Discovery* **2002**, *1*, 727–730; c) A. P. Russ, S. Lampel, *Drug Discovery Today*, **2005**, *10*, 1607–1610; d) R. Santos, O. Ursu, A. Gaulton, A. P. Bento, R. S. Donadi, C. G. Bologa, A. Karlsson, B. Al-Lazikani, A. Hersey, T. I. Oprea, J. P. Overington, *Nat. Rev. Drug Discovery* **2017**, *16*, 19–34.
- [2] a) K. M. Stewart, K. L. Horton, S. O. Kelley, *Org. Biomol. Chem.* **2008**, *6*, 2242–2255; b) M. Pooga, Ü. Langel in *Cell Preserv. Technol.*, (Eds.: Ü. Langel), Springer Science+Business, New York, **2015**, pp. 3–28; c) F. Milletti, *Drug Discovery Today* **2012**, *17*, 850–860; d) V. Biju, T. Itoh, M. Ishikawa, *Chem. Soc. Rev.* **2010**, *39*, 3031–3056; e) T. Serdiuk, I. Bakanovich, V. Lysenko, S. A. Alekseev, V. A. Skryshevsky, S. Afonin, E. Berger, A. Geloën, I. V. Komarov, *RSC Adv.* **2015**, *5*, 20498–20502.
- [3] a) C. Bechara, S. Sagan, *FEBS Lett.* **2013**, *587*, 1693–1702; b) D. M. Copolovici, K. Langel, E. Eriste, Ü. Langel, *ACS Nano* **2014**, *8*, 1972–1994; c) J. Fominaya, J. Bravo, A. Rebollo, *Ther. Delivery* **2015**, *6*, 1171–1194; d) W. B. Kauffman, T. Fuselier, J. He, W. C. Wimley, *Trends Biochem. Chem.* **2015**, *40*, 749–764; e) A. Komin, L. M. Russell, K. A. Hristova, P. C. Searson, *Adv. Drug Delivery Rev.* **2017**, *110*, 52–64; f) R. Rezgui, K. Blumer, G. Yeoh-Tan, A. J. Trexler, M. Magzoub, *Biochim. Biophys. Acta Biomembr.* **2016**, *1858*, 1499–1506; g) F. Illien, N. Rodriguez, M. Amoura, A. Joliot, M. Pallerla, S. Cribier, F. Burlina, S. Sagan, *Sci. Rep.* **2016**, *6*, 36938; h) G. Guidotti, L. Brambilla, D. Rossi, *Trends Pharmacol. Sci.* **2017**, *38*, 406–424; i) L. Peraro, J. Kritzer, *Angew. Chem. Int. Ed.* **2018**, *57*, 11868–11881; *Angew. Chem.* **2018**, *130*, 12042–12057; j) H. Derakhshankhah, S. Jafari, *Biomed. Pharmacother.* **2018**, *108*, 1090–1096; k) L. Peraro, K. L. Deprey, M. K. Moser, Z. Zou, H. L. Ball, B. Levine, J. A. Kritzer, *J. Am. Chem. Soc.* **2018**, *140*, 11360–11369; l) A. Méndez-Ardoy, I. Lostalé-Seijo, J. Montenegro, *ChemBioChem* **2019**, *20*, 488–498.
- [4] a) A. D. Frankel, C. O. Pabo, *Cell* **1988**, *55*, 1189–1193; b) Collado Camps, R. Brock, *Bioorg. Med. Chem.* **2018**, *26*, 2780–2787.
- [5] A. F. B. Räder, F. Reichart, M. Weinmüller, H. Kessler, *Bioorg. Med. Chem.* **2018**, *26*, 2766–2773.
- [6] a) A. Zorzi, K. Deyle, C. Heinis, *Curr. Opin. Chem. Biol.* **2017**, *38*, 24–29; b) Z. Qian, P. G. Dougherty, D. Pei, *Curr. Opin. Chem. Biol.* **2017**, *38*, 80–86.
- [7] a) M. J. Klein, S. Schmidt, P. Wadhwani, J. Bürck, J. Reichert, S. Afonin, M. Berditsch, T. Schöber, R. Brock, M. Kansy, Anne S. Ulrich, *J. Med. Chem.* **2017**, *60*, 8071–8082; b) T. K. Sawyer, A. W. Partridge, H. Y. K. Kaan, Y. C. Juang, S. Lim, C. Johannes, T. Y. Yuen, C. Verma, S. Kannan, P. Aronica, Y. S. Tanc, B. Sherborne, S. Ha, J. Hochman, S. Chen, L. Surdi, A. Peier, B. Sauvagnat, P. J. Dandliker, C. J. Brown, S. Ng, F. Ferrer, D. P. Lane, *Bioorg. Med. Chem.* **2018**, *26*, 2807–2815.
- [8] a) S. T. Henriques, D. J. Craik, *Drug Discovery Today* **2010**, *15*, 57–64; b) D. J. Craik, J. Du, *Curr. Opin. Chem. Biol.* **2017**, *38*, 8–16; c) C. K. Wang, D. J. Craik, *Nat. Chem. Biol.* **2018**, *14*, 417–427.
- [9] a) M. R. Sebastiano, B. C. Doak, M. Backlund, V. Poongavanam, B. Over, G. Ermondi, G. Caron, P. Matsson, J. Kihlberg, *J. Med. Chem.* **2018**, *61*, 4189–4202; b) M. Tyagi, V. Poongavanam, M. Lindhagen, A. Pettersen, P. Sjö, S. Schiesser, J. Kihlberg, *Org. Lett.* **2018**, *20*, 5737–5742.
- [10] S. Dissanayake, W. A. Denny, S. Gamage, V. Sarojini, *J. Controlled Release* **2017**, *250*, 62–76.
- [11] a) Y. Gilad, M. Firer, G. Gellerman, *Biomedicine* **2016**, *4*, 11; b) V. Le Joncour, P. Laakkonen, *Bioorg. Med. Chem.* **2018**, *26*, 2797–2806.
- [12] S. A. Bode, D. W. P. M. Löwik, *Drug Discovery Today Technol.* **2017**, *26*, 33–42.
- [13] a) R. R. Sawant, N. R. Patel, V. P. Torchilin, *Eur. J. Nanomed.* **2013**, *5*, 141–158; b) L. Fei, L. P. Yap, P. S. Conti, W. C. Shen, J. L. Zaro, *Biomaterials* **2014**, *35*, 4082–4087; c) C. Sun, W. C. Shen, J. Tu, J. L. Zaro, *Mol. Pharm.* **2014**, *11*, 1583–1590; d) H. Cheng, J. Y. Zhu, X. D. Xu, W. X. Qiu, Q. Lei, K. Han, Y. J. Cheng, X. Z. Zhang, *ACS Appl. Mater. Interfaces* **2015**, *7*, 16061–16069; e) K. Kurrikoff, M. Gestin, Ü. Langel, *Expert Opin. Drug Delivery* **2016**, *13*, 373–387.
- [14] a) R. Weissleder, *Nat. Biotechnol.* **2001**, *19*, 316–317; b) C. Brieke, F. Rohrbach, A. Gottschalk, G. Mayer, A. Heckel, *Angew. Chem. Int. Ed.* **2012**, *51*, 8446–8476; *Angew. Chem.* **2012**, *124*, 8572–8604; c) S. Samanta, A. A. Beharry, O. Sadovski, T. M. McCormick, A. Babalhavaej, V. Tropepe, G. A. Woolley, *J. Am. Chem. Soc.* **2013**, *135*, 9777–9784; d) R. Siewertsen, H. Neumann, B. Buchheim-Stehn, R. Herges, C. Näther, F. Renth, F. Temps, *J. Am. Chem. Soc.* **2009**, *131*, 15594–15595.
- [15] a) G. Mayer, A. Hechel, *Angew. Chem. Int. Ed.* **2006**, *45*, 4900–4921; *Angew. Chem.* **2006**, *118*, 5020–5042; b) H. M. Lee, D. R. Larson, D. S. Lawrence, *ACS Chem. Biol.* **2009**, *4*, 409–427.
- [16] a) Y. Shamay, L. Adar, G. Ashkenasy, A. David, *Biomaterials* **2011**, *32*, 1377–1386; b) M. B. Hansen, E. Van Gaal, I. Minten, G. Storm, J. C. M. Van Hest, D. W. P. M. Löwik, *J. Controlled Release* **2012**, *164*, 87–94.
- [17] a) W. A. Velema, J. P. van der Berg, M. J. Hansen, W. Szymanski, A. J. M. Driessen, B. L. Feringa, *Nat. Chem.* **2013**, *5*, 924–928; b) W. A. Velema, W. Szymanski, B. L. Feringa, *J. Am. Chem. Soc.* **2014**, *136*, 2178–2191; c) J. Broichhagen, J. A. Frank, D. Trauner, *Acc. Chem. Res.* **2015**, *48*, 1947–1960; d) M. M. Lerch, M. J. Hansen, G. M. van Dam, W. Szymanski, B. L. Feringa, *Angew. Chem. Int. Ed.* **2016**, *55*, 10978–10999; *Angew. Chem.* **2016**, *128*, 11140–11163; e) K. Hüll, J. Morstein, D. Trauner, *Chem. Rev.* **2018**, *118*, 10710–10747; f) M. W. H. Hoorens, W. Szymanski, *Trends Biochem. Sci.* **2018**, *43*, 567–575.
- [18] a) W. Szymanski, J. M. Beierle, H. A. V. Kistemaker, W. A. Velema, B. L. Feringa, *Chem. Rev.* **2013**, *113*, 6114–6178; b) Z. L. Pianowski, *Chem. Eur. J.* **2019**, DOI 10.1002/chem.201805814.
- [19] A. Prestel, H. M. Möller, *Chem. Commun.* **2016**, *52*, 701–704.
- [20] R. J. Mart, R. K. Allemann, *Chem. Commun.* **2016**, *52*, 12262–12277.
- [21] L. Nevola, A. Martín-Quirós, K. Eckelt, N. Camarero, S. Tosi, A. Llobet, E. Giral, P. Gorostiza, *Angew. Chem. Int. Ed.* **2013**, *52*, 7704–7708; *Angew. Chem.* **2013**, *125*, 7858–7862.
- [22] G. C. Kim, J. H. Ahn, J. H. Oh, S. Nam, S. Hyun, J. Yu, Y. Lee, *Biomacromolecules* **2018**, *19*, 2863–2869.
- [23] a) G. Tünnemann, R. M. Martin, S. Haupt, C. Patsch, F. Edenhofer, M. C. Cardoso, *FASEB J.* **2006**, *20*, 1775–1784; b) D. Birch, M. V. Christensen, D. Staerk, H. Franzky, H. M. Nielsen, *Biochim. Biophys. Acta Biomembr.* **2017**, *1859*, 2483–2494; c) S. F. Hedegaard, M. S. Derbas, T. K. Lind, M. R. Kasimova, M. V. Christensen, M. H. Michaelson, R. A. Campbell, L. Jorgensen, H. Franzky, M. Cárdenas, *Sci. Rep.* **2018**, *8*, 1–14; d) É. Kiss, G. Gyulai, E. Pári, K. Horváti, S. Bösze, *Amino Acids* **2018**, *50*, 1557–1571.
- [24] a) O. Babii, S. Afonin, M. Berditsch, S. Reier, P. K. Mykhailiuk, V. S. Kubyskhin, T. Steinbrecher, A. S. Ulrich, I. V. Komarov, *Angew. Chem. Int. Ed.* **2014**, *53*, 3392–3395; *Angew. Chem.* **2014**, *126*, 3460–3463; b) O. Babii, S. Afonin, L. V. Garmanchuk, V. V. Nikulina, T. V. Nikolaienko, O. V. Storozhuk, D. V. Shelest, O. I. Dasyukevich, L. I. Ostapchenko, V. Iurchenko, *Angew. Chem. Int. Ed.* **2016**, *55*, 5493–5496; *Angew. Chem.*

- 2016, 128, 5583–5586; c) I. V. Komarov, S. Afonin, O. Babii, T. Schober, A. S. Ulrich, *Chem. Eur. J.* **2018**, 24, 1–11; d) O. Babii, S. Afonin, A. Y. Ishchenko, T. Schober, A. O. Negelia, G. M. Tolstanova, L. V. Garmanchuk, L. I. Ostapchenko, I. V. Komarov, A. S. Ulrich, *J. Med. Chem.* **2018**, 61, 10793–10813.
- [25] Z. Qian, A. Martyna, R. L. Hard, J. Wang, G. Appiah-Kubi, C. Coss, M. A. Phelps, J. S. Rossman, D. Pei, *Biochemistry* **2016**, 55, 2601–2612.
- [26] Z. Qian, J. R. Larochelle, B. Jiang, W. Lian, R. L. Hard, N. G. Selner, R. Luechapanichkul, A. M. Barrios, D. Pei, *Biochemistry* **2014**, 53, 4034–4046.
- [27] D. Meyer, C. Mutschler, I. Robertson, A. Batt, C. Tatko, *J. Pept. Sci.* **2013**, 19, 277–282.
- [28] M. L. Jobin, M. Blanchet, S. Henry, S. Chaignepain, C. Manigand, S. Castano, S. Lecomte, F. Burlina, S. Sagan, I. D. Alves, *Biochim. Biophys. Acta Biomembr.* **2015**, 1848, 593–602.
- [29] E. Danelius, M. Pettersson, M. Bred, J. Min, M. B. Waddell, R. K. Guy, M. Grøtli, M. Erdelyi, *Org. Biomol. Chem.* **2016**, 14, 10386–10393.
- [30] G. Lättig-Tünnemann, M. Prinz, D. Hoffmann, J. Behlke, C. Palm-Apergi, I. Morano, H. D. Herce, M. C. Cardoso, *Nat. Commun.* **2011**, 2, 453.
- [31] H. Yamashita, T. Kato, M. Oba, T. Misawa, T. Hattori, N. Ohoka, M. Tanaka, M. Naito, M. Kurihara, Y. Demizu, *Sci. Rep.* **2016**, 6, 2–9.
- [32] a) Y. Takechi-Haraya, R. Nadaï, H. Kimura, K. Nishitsuji, K. Uchimura, K. Sakai-Kato, K. Kawakami, A. Shigenaga, T. Kawakami, A. Otaka, H. Hojo, N. Sakashita, H. Saito, *Biochim. Biophys. Acta Biomembr.* **2016**, 1858, 1339–1349; b) Y. A. Nagel, P. S. Raschle, H. Wennemers, *Angew. Chem. Int. Ed.* **2017**, 56, 122–126; *Angew. Chem.* **2017**, 129, 128–132.
- [33] a) K. M. Biswas, D. R. de Vido, J. G. Dorsey, *J. Chromatogr. A*, **2003**, 1000, 637–655; b) J. M. Kovacs, C. T. Mant, R. S. Hodges, *Biopolymers* **2006**, 84, 283–297.
- [34] a) G. Tünnemann, G. Ter-Avetisyan, R. M. Martin, M. Stöckl, A. Herrmann, M. C. Cardoso, *J. Pept. Sci.* **2008**, 14, 469–476; b) C. P. Cerrato, K. Künnapuu, Ü. Langel, *Expert Opin. Drug Delivery* **2017**, 14, 245–255.
- [35] a) J. Hed, G. Hallden, S. G. O. Johansson, P. Larsson, *J. Immunol. Methods* **1987**, 101, 119–125; b) D. Raucher, A. Chilkoti, *Cancer Res.* **2001**, 61, 7163–7170.
- [36] I. V. Komarov, S. Afonin, O. Babii, T. Schober, A. S. Ulrich, *Chem. Eur. J.* **2018**, 24, 11245–11254.
- [37] a) S. Jin, N. Kedia, E. Illes-Toth, I. Haralampiev, S. Prisner, A. Herrmann, E. E. Wanker, J. Bieschke, *J. Biol. Chem.* **2016**, 291, 19590–19606; b) L. D. Evans, T. Wassmer, G. Fraser, J. Smith, M. Perkinson, A. Billinton, F. J. Livesey, *Cell Rep.* **2018**, 22, 3612–3624.

Manuscript received: January 22, 2019

Revised manuscript received: April 17, 2019

Accepted manuscript online: May 4, 2019

Version of record online: May 22, 2019